

University of Groningen

Magnetic and magnetoelectric properties of Ho₂BaNiO₅

Nenert, G.; Palstra, Thomas

Published in:
Physical Review. B: Condensed Matter and Materials Physics

DOI:
[10.1103/PhysRevB.76.024415](https://doi.org/10.1103/PhysRevB.76.024415)

IMPORTANT NOTE: You are advised to consult the publisher's version (publisher's PDF) if you wish to cite from it. Please check the document version below.

Document Version
Publisher's PDF, also known as Version of record

Publication date:
2007

[Link to publication in University of Groningen/UMCG research database](#)

Citation for published version (APA):
Nenert, G., & Palstra, T. T. M. (2007). Magnetic and magnetoelectric properties of Ho₂BaNiO₅. *Physical Review. B: Condensed Matter and Materials Physics*, 76(2), [024415]. DOI: 10.1103/PhysRevB.76.024415

Copyright

Other than for strictly personal use, it is not permitted to download or to forward/distribute the text or part of it without the consent of the author(s) and/or copyright holder(s), unless the work is under an open content license (like Creative Commons).

Take-down policy

If you believe that this document breaches copyright please contact us providing details, and we will remove access to the work immediately and investigate your claim.

Downloaded from the University of Groningen/UMCG research database (Pure): <http://www.rug.nl/research/portal>. For technical reasons the number of authors shown on this cover page is limited to 10 maximum.

Magnetic and magnetoelectric properties of $\text{Ho}_2\text{BaNiO}_5$

G. Nénert and T. T. M. Palstra

Solid State Chemistry Laboratory, Zernike Institute for Advanced Materials, University of Groningen, Nijenborg 4, 9747 AG Groningen, The Netherlands

(Received 5 April 2007; revised manuscript received 11 June 2007; published 11 July 2007)

The compounds $R_2\text{BaNiO}_5$, with R a rare earth, exhibit low dimensional magnetism including a Haldane gap, originating from Ni^{2+} chains. In these compounds, the rare-earth ions give rise to three-dimensional antiferromagnetic ordering which does not eliminate the Haldane-like behavior. We study here the interplay between magnetic and dielectric properties of $\text{Ho}_2\text{BaNiO}_5$ on a polycrystalline sample. We show that a linear magnetoelectric effect exists in this compound. We discuss our results in the light of the rich magnetic phase diagram of $\text{Ho}_2\text{BaNiO}_5$.

DOI: 10.1103/PhysRevB.76.024415

PACS number(s): 75.30.Kz, 77.80.Bh, 64.70.Kb

I. INTRODUCTION

Interest in low dimensional magnetism was greatly renewed by the theoretical work of Haldane, who predicted that an integer-spin Heisenberg antiferromagnetic chain should have a singlet ground state, and a gap in the magnetic spectrum.¹ Several examples of quasi-one-dimensional systems with a Haldane gap have been studied by now (see Ref. 2 and references therein). Most of the work has been carried out on organometallic compounds.³

Darriet and Regnault⁴ and DiTusa *et al.*⁵ were the first to observe a Haldane gap in a metal oxide compound, namely, Y_2BaNiO_5 . The $R_2\text{BaNiO}_5$ (R =rare earth or Y) oxides present interesting structural and magnetic properties due to the fact that their structure possesses a strong one-dimensional (1D) character.^{6,7} As a function of R and the synthesis conditions, the $R_2\text{BaNiO}_5$ family can crystallize in two different polymorphs: $Pnma$ (no. 62) and $Immm$ (no. 71).^{8,9} The members in which we are interested have the $Immm$ symmetry. The main structural feature is the presence of 1D chains of NiO_6 octahedra along the a axis. The octahedra are strongly distorted with a very short $\text{Ni-O}_{\text{apical}}$ distance ($\approx 1.88 \text{ \AA}$), and a longer $\text{Ni-O}_{\text{basal}}$ distance ($\approx 2.18 \text{ \AA}$) (see Fig. 1).

In particular, the $R_2\text{BaNiO}_5$ family is of interest from a magnetic point of view, due to the fact that the onset of 3D long-range magnetic order does not eliminate the Haldane-like behavior above and below the Néel temperature.¹⁰ Our motivation in studying the Ho member of this family was triggered by two reasons: the existence of two field induced phase transitions at low temperature and the possible existence of magnetoelectricity. We will show in a first part that we predict the presence of a linear magnetoelectric effect based on symmetry analysis. From this prediction, we have synthesized the compound and studied its magnetic properties. We finally demonstrate experimentally the presence of an induced polarization by application of a magnetic field (linear magnetoelectric effect) on a polycrystalline sample. We discuss the magnetic field behavior of the induced polarization in the light of the two unusual field induced phase transitions.

II. MAGNETIC SYMMETRY ANALYSIS

García-Matres *et al.* have studied the magnetic structures of most of the members of the $R_2\text{BaNiO}_5$ family using neu-

tron powder diffraction ($R=\text{Nd, Tb, Dy, Ho, Er, and Tm}$).¹¹ Below T_N , $\text{Ho}_2\text{BaNiO}_5$ orders magnetically with a magnetic wave vector $\vec{k}=(1/2, 0, 1/2)$. The Ni atoms occupy the Wyckoff position $2a$ and the Ho atoms occupy the Wyckoff position $4j$ with $z \approx 0.202$. The authors determined the point group of the little group G_k being $2/m$. Using group theoretical methods, they determined that $\text{Ho}_2\text{BaNiO}_5$ could be described by the B_g representation of the little group $2/m$. Consequently, the magnetic moments of Ni and Ho ions are within the ac plane. The easiest way to describe the magnetic structure is to work in the enlarged unit cell. Using the program ISOTROPY,¹² an enlargement of the unit cell by a vector $(1/2, 0, 1/2)$ gives rise to the space group $Cmmm$ (no. 65) with $\vec{a}'=2\vec{c}$, $\vec{b}'=2\vec{a}$, and $\vec{c}'=\vec{b}$. The new Wyckoff positions for Ni are (in the $Cmmm$ setting) $2a$, $2b$, and $4f$. The new Wyckoff positions for Ho are $8p$, and two times $4h$ with different x coordinate in $Cmmm$ setting.

We know from the work of García-Matres and co-workers^{11,13} that the magnetic moments of Ni and Ho at 1.5 K are $\vec{S}_{\text{Ni}}=[0.58(9), 0, -1.26(4)]$ and $\vec{S}_{\text{Ho}}=[0.12(5), 0, 9.06(4)]$, respectively. We consider only one propagation vector which defines the magnetic structure. Thus we can relate any magnetic moment in the structure by

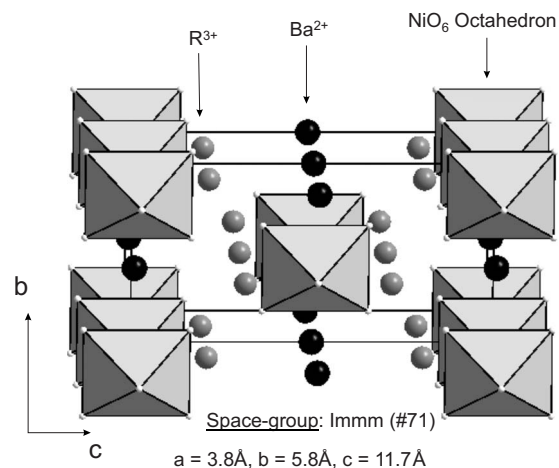


FIG. 1. Crystallographic structure of the $R_2\text{BaNiO}_5$ in the space group $Immm$. The cell parameters are $a \approx 3.8 \text{ \AA}$, $b \approx 5.8 \text{ \AA}$, and $c \approx 11.3 \text{ \AA}$ for small R and $c \approx 11.7 \text{ \AA}$ for large R .

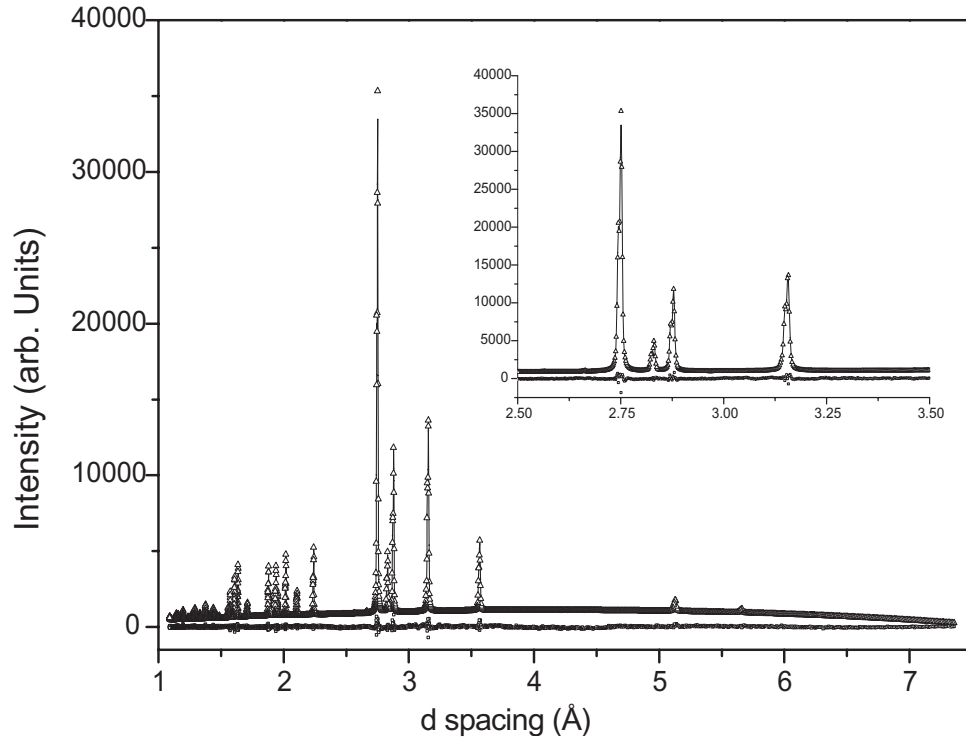


FIG. 2. Refinement of the crystal structure of $\text{Ho}_2\text{BaNiO}_5$ on a powder sample. The refinement was carried with $Immm$ symmetry giving rise to the following statistics: $GoF=1.51$, $wR_p=3.28\%$, and $R_p=3.94\%$. Cell parameters: $a=3.76\ 010(5)\ \text{\AA}$, $b=5.758\ 71(7)\ \text{\AA}$, $c=11.3275(1)\ \text{\AA}$ at room temperature.

$$\vec{S}_n = \vec{S}_k \exp(-i2\pi\vec{k} \cdot \vec{R}_n), \quad (1)$$

where \vec{S}_n is the magnetic moment of the atom considered attached to the lattice point \vec{R}_n for a magnetic wave vector \vec{k} . We investigate the eight axial vector representations of the symmetry elements (we deal here with spins) of the space-group $Cmmm$ (in the enlarged unit cell). We find out that the only symmetry elements which remain are the two fold axis along y (in $Cmmm$ symmetry) and the mirror m_{xy} (in $Cmmm$ symmetry) which is primed. Consequently, the magnetic point group describing the magnetic order under T_N is $2/m'$. According to Ref. 14 this compound may present a linear magnetoelectric effect. This prediction has been the motivation for an experimental investigation of $\text{Ho}_2\text{BaNiO}_5$.

III. SYNTHESIS AND CHARACTERIZATION

The synthesis of $\text{Ho}_2\text{BaNiO}_5$ was already reported.^{9,11,13} We follow a similar procedure for the synthesis of our sample. $\text{Ho}_2\text{BaNiO}_5$ was prepared as polycrystalline material by solid state reaction from stoichiometric mixtures of analytical grade Ho_2O_3 (dried at $1000\ ^\circ\text{C}$ overnight prior to use), NiO (99.999%), and BaCO_3 . The sample was ground, pelletized, and heated in air overnight at 900 , 950 , 1050 , and $1100\ ^\circ\text{C}$ until reaching x-ray pure sample. After each thermal treatment, the reaction products were reground and pelletized before starting the next treatment.

The quality of the sample was checked by means of powder x-ray diffraction using a Bruker D8 Advance diffractometer with an energy dispersive detector. Refinement of the

powder data has been carried out using the program GSAS.¹⁵ We use the peak profile function of type 2 in GSAS. Only three parameters have been used to describe the peak shape with one Gaussian parameter, one Lorentzian parameter, and the shift. The results of the refinement are presented in Fig. 2 and in Table I. We obtain very good refinement of the structure with the following statistics: $GoF=1.51$, $wR_p=3.28\%$, and $R_p=3.94\%$ with cell parameters $a=3.760\ 10(5)\ \text{\AA}$, $b=5.758\ 71(7)\ \text{\AA}$, $c=11.3275(1)\ \text{\AA}$ at room temperature.

IV. MAGNETIC PROPERTIES

The magnetic properties have been investigated for two reasons: the magnetoelectric effect is dependent on the magnetic properties and two field induced phase transitions have been reported for $\text{Ho}_2\text{BaNiO}_5$. Checking for the existence of such transition is a good way to further investigate the qual-

TABLE I. Crystallographic coordinates extracted from the Rietveld refinement carried out on x-ray powder diffraction using the space group $Immm$ at room temperature.

Atom	Wyckoff	x	y	z	U_{iso}
Ho	$4j$	0.5	0	0.7977(1)	0.0473(7)
Ba	$2c$	0.5	0.5	0	0.0490(8)
Ni	$2a$	0	0	0	0.049(1)
O_1	$8l$	0	0.766(1)	0.8500(5)	0.058(2)
O_2	$2b$	0	0.5	0.5	0.041(5)

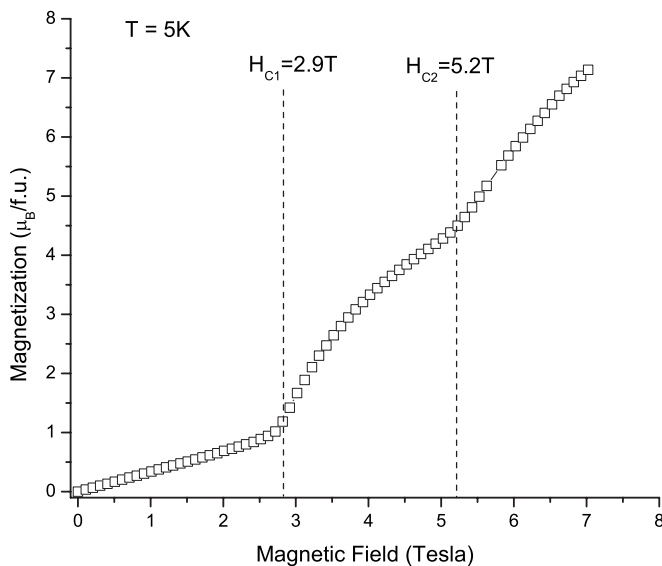


FIG. 3. Magnetic field dependence of the magnetization measured on a pellet of $\text{Ho}_2\text{BaNiO}_5$ at 5 K. Two noticeable magnetic induced transitions are at $H_{C1}=2.9$ T and at $H_{C2}=5.2$ T.

ity of the sample, especially in terms of phase purity.

We present in Fig. 3 the field dependence of the magnetization measured at $T=5$ K in order to confirm the experimental observations.^{9,11,13} We confirm the two field induced phase transitions at a slightly different value for H_{C2} (5.2 T vs 5.4 T) and exactly the same for H_{C1} (2.9 T).

The magnetization for $\text{Ho}_2\text{BaNiO}_5$ reaches $\approx 1\mu_B$ at H_{C1} and $\approx 4.5\mu_B$ at H_{C2} per formula unit. From neutron measurements in zero magnetic field,¹³ the Ni moments are rotated 26° from the c axis to the a axis, and the Ho moment is almost collinear with the c axis at 1.5 K (0.7°). The Ni and Ho moments reach $1.4\mu_B$ and $9\mu_B$ at 1.5 K, respectively. Thus we observe that even at H_{C2} , we are still far from the saturated value of the magnetic moment of Ho. This is in contrast with $\text{Nd}_2\text{BaNiO}_5$. In this material, a full saturation of the rare-earth moment is reached at H_{C2} ,¹⁶ while this is not the case for Ho in $\text{Ho}_2\text{BaNiO}_5$. From neutron diffraction, we expect that the scenario for Nd would also hold for Ho since both rare earths order along the c axis. Experiments on single crystal of $\text{Ho}_2\text{BaNiO}_5$ could clarify the reasons for this discrepancy. In addition to the magnetization vs magnetic field, we measure also the temperature dependence of the magnetic susceptibility of a $\text{Ho}_2\text{BaNiO}_5$ pellet. The results are presented in Figs. 4 and 5.

The magnetic susceptibility data present the common features of the $R_2\text{BaNiO}_5$ family. There is a broad maximum at around 30 K characteristic for all the family. Indeed, this broad maximum (maximum at χ_{max}) is always present below T_N for any R (e.g., $\text{Er}_2\text{BaNiO}_5$, $T_{max}=16$ K, and $T_N=33$ K).¹⁷ From neutron diffraction, it has been shown that there is a change of slope of the Ho magnetic moment around 30 K corresponding to χ_{max} in the magnetic susceptibility data.¹³ In low-dimensional magnetic systems a maximum in magnetic susceptibility is not related to the 3D antiferromagnetic ordering. The magnetic data, such as reported in Fig. 4, were analyzed as presented in Fig. 6 for magnetic fields of several

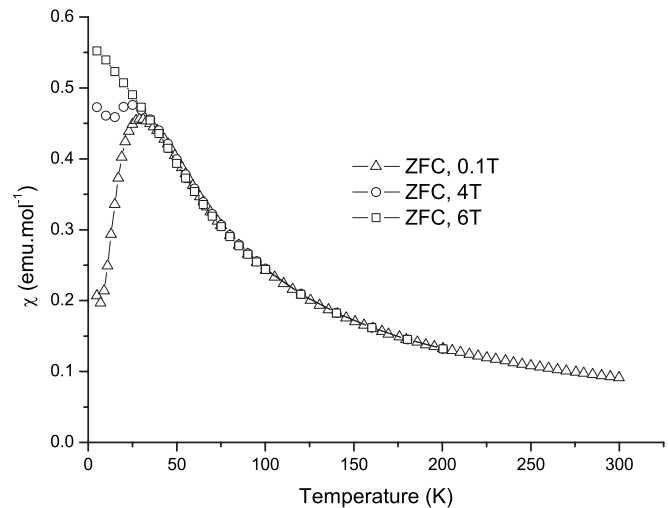


FIG. 4. Magnetic susceptibility measured on a $\text{Ho}_2\text{BaNiO}_5$ pellet in zero field cooled mode function for different applied magnetic fields: 0.1 T (triangles), 4 T (circles), and 6 T (squares).

T. However, no signature of a phase transition could be observed.

In Fig. 5, we present the inverse susceptibility of a polycrystalline sample of $\text{Ho}_2\text{BaNiO}_5$ measured in zero field cooled mode with a magnetic field of 0.01 T. We could fit the data in the paramagnetic phase using a Curie-Weiss dependence defined by $\frac{1}{\chi} = \frac{T+\theta}{C}$ between 200 and 300 K. We find that $\text{Ho}_2\text{BaNiO}_5$ exhibits ferromagnetic interactions since θ is positive ($\theta=10.8$ K). In addition, the value of the Curie constant $C=27.8$ emu K mol^{-1} is in good agreement with the theoretical value of 28. It should be noted that at all temperatures the magnetic susceptibility is dominated by the contribution of the Ho^{3+} moments ($p_{eff}=10.4\mu_B$, $C_{2\times\text{Ho}^{3+}}=27$ emu K mol^{-1}) being much larger than the contribution of the Ni^{2+} moments ($p_{eff}=2.8\mu_B$, $C_{\text{Ni}^{2+}}=1$ emu K mol^{-1}). This means that in the paramagnetic regime the Ni^{2+} contri-

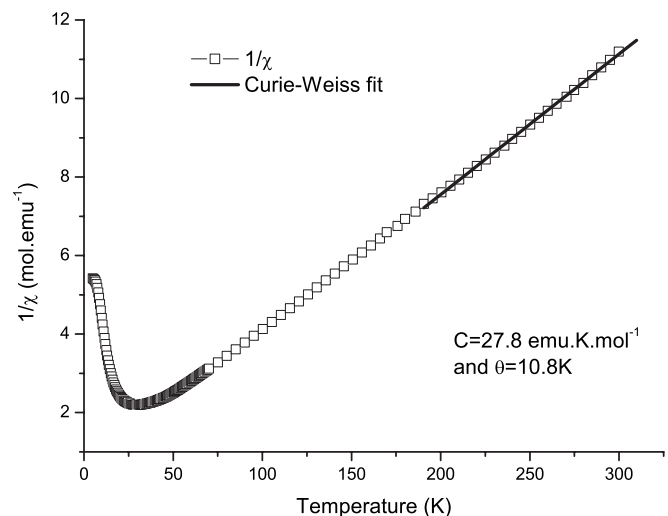


FIG. 5. Inverse magnetic susceptibility measured on a pellet of $\text{Ho}_2\text{BaNiO}_5$ in zero field cooled mode with 0.01 T. The line is a fit of the Curie-Weiss function using $\frac{1}{\chi} = \frac{T+\theta}{C}$.

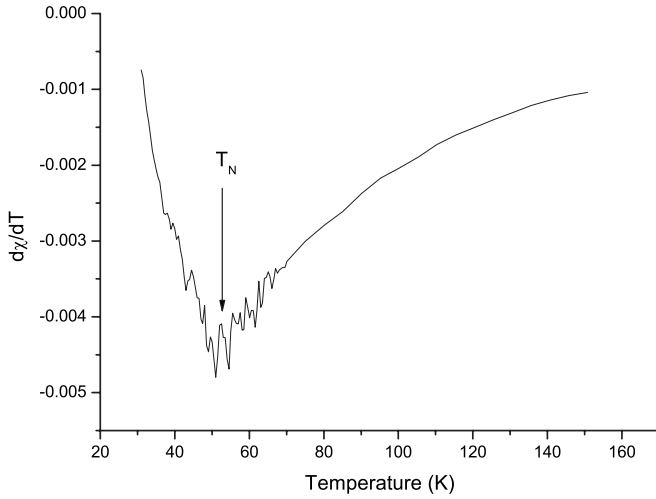


FIG. 6. $d\chi/dT$ vs temperature for an applied field of 0.01 T. The arrow indicates the Néel temperature in agreement with the literature (Refs. 11, 13, and 17).

bution is only about 4% of the total susceptibility.

Considering the derivative $d\chi/dT$, we notice an anomaly around 50 K in agreement with the reported Néel temperature of $T_N=53$ K (Refs. 11, 13, and 17) (see Fig. 6). Consequently, we ascribe this anomaly as the signature for the Néel temperature. The insufficient accuracy of our data for higher magnetic fields does not allow, even by plotting $d\chi/dT$, the determination of the magnetic ordering temperature. In first approximation, we assume that T_N does not change.

In Fig. 4, we can observe that the decrease below χ_{max} disappears when applying a magnetic field of 6 T. As the susceptibility is dominated by the Ho contribution, this decrease should be associated with the magnetic behavior of the Ho spins. There can be several reasons for this decrease: (i) the magnetic ordering of the Ho sublattice; (ii) the low-dimensional behavior of the Ho sublattice, or (iii) a coupling of the Ho^{3+} spins to the Ni^{2+} -Haldane system. We consider the first possibility unlikely because this would not lead to a suppression below 30 K but already below $T_N \approx 53$ K.¹³ The second option arises from the large moment for Ho for which a field of 6 T represents a significant magnetic energy compared with the magnetic interactions. Nevertheless, we adopt the suggestion by Zheludev *et al.*¹⁸ They argue that there exists significant coupling of local crystal field excitations of the rare-earth ions to the Haldane-gap excitations of the Ni sublattice. In such case the low-temperature behavior of the susceptibility may be determined by excitations of the Ho sublattice, being coupled to the Ni-sublattice system, which exhibits excitations across the Haldane gap Δ . Modeling the magnetic susceptibility by a temperature independent term and a Haldane-gap term $\frac{\exp(-\Delta/T)}{\sqrt{T}}$,¹⁹ we extract from our magnetic susceptibility data below 15 K a value of $\Delta \approx 42$ K which is significantly lower than the value reported for $\text{Nd}_2\text{BaNiO}_5$ ($\Delta=127$ K) (Ref. 20) or for Y_2BaNiO_5 ($\Delta=100$ K) (Ref. 4) (see Fig. 7).

The dependence of the Néel temperature of this family as function of the ionic radius suggests the influence of the volume, as well as the value of gJ , in the magnetic order.¹¹

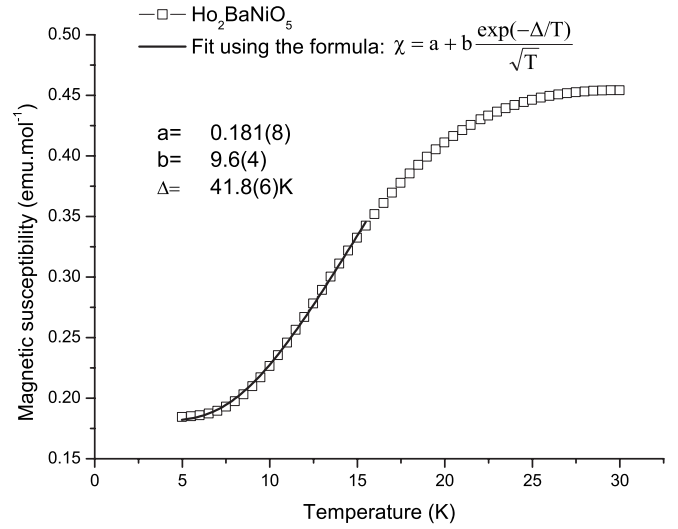


FIG. 7. Estimation of the Haldane gap in $\text{Ho}_2\text{BaNiO}_5$ by modeling the low temperature data with $\chi = a + b \frac{\exp(-\Delta/T)}{\sqrt{T}}$. We use the temperature range 5–15 K.

For a Haldane system, the value of the gap Δ depends on the value of J . The value of the gap for $\text{Ho}_2\text{BaNiO}_5$ is reduced by a factor 2 compared to other known $R_2\text{BaNiO}_5$. Such reduction of the gap could be due to different reasons: (i) a significant difference in the Ni-Ni distances for $\text{Ho}_2\text{BaNiO}_5$ compared to the other rare earths; (ii) an interchain coupling much larger in $\text{Ho}_2\text{BaNiO}_5$ which would renormalize the value of the gap. The first possibility is unlikely due to the fact that the Ni-Ni distance [cell parameter $a=d$ (Ni-Ni)] varies only by few percent over the different ionic radius (see Fig. 8).

If we assume that J does not change much between different members of the $R_2\text{BaNiO}_5$ family, which is true at least for Tb, Dy, Ho, Er, and Tm,¹¹ the value of the Haldane gap Δ should vary in an opposite fashion to the Néel temperature. We see in Fig. 8 that the Néel temperature increases linearly between Yb and Dy. Thus we believe that the reason for a reduced Haldane gap in $\text{Ho}_2\text{BaNiO}_5$ is likely due to a

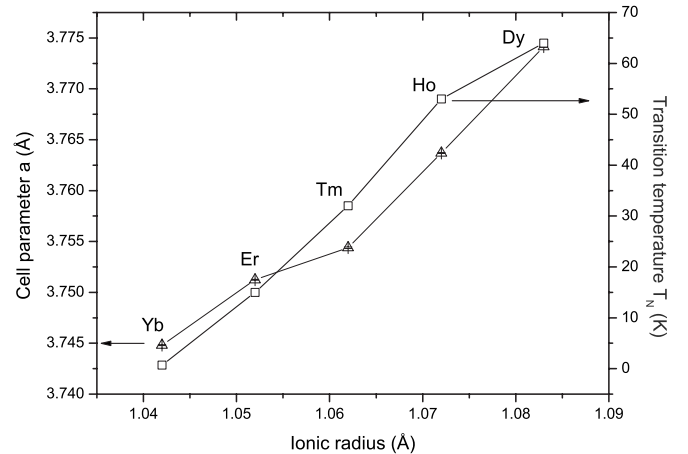


FIG. 8. The Néel temperature and the a cell parameter of some $R_2\text{BaNiO}_5$ from Ref. 7.

renormalization originating from the onset of a long-range magnetic ordering.

We believe that for $T \ll \Delta$, the magnetic susceptibility exhibits Haldane behavior (see Fig. 7) originating from the Ho spins, being coupled by exchange to the Ni sublattice. Thus the disappearance of the decrease in χ below χ_{max} can be associated with the closure of the Haldane gap by a magnetic field, or with a change in the coupling of the Ho spins to the Ni spins. We do not know the influence of the external magnetic field on the staggered exchange field acting on the Ni chains due to the Ho sublattice magnetization. In zero field, the staggered exchange field is about 35 T.²⁰ Therefore we believe that an external magnetic field of $6T \ll 35T$ does not close the Haldane gap.

V. MAGNETOELECTRICITY

Now that we have investigated the magnetic properties of $\text{Ho}_2\text{BaNiO}_5$, we will show that we could induce a finite polarization in a magnetic field. The polarization was measured in a magnetic field. For each measurement, we cooled down the sample to 5 K starting from 90 K ($T \gg T_N$). During the cooling process, we applied the magnetic field perpendicular to the electric field (magnetolectric annealing). We used two different electric fields: 3.15 kV/cm (175 V) and 4.5 kV/cm (250 V). At 5 K, we removed the electric field and kept the magnetic field. The induced polarization was measured upon heating by integrating the pyroelectric current. The electric field was generated using a Keithley 237 high voltage source measure unit. The pyroelectric current was measured using a Keithley 617 programmable electrometer. The sample used was a sintered pellet polished down to 0.55 mm thickness with 0.5 mm² contact area. In general, a polycrystalline sample has random orientations of the crystallographic axes. Applying an electric field will generate a polarization in accordance with the component of the electric field along the polar axis. Consequently in the measurements presented below the absolute value of the pyroelectric current do not reflect the value corresponding to a monodomain single crystal. This picture is further complicated by the eventual presence of domains of the various grains and the high anisotropy of the material (one-dimensional system) The temperature scale is accurate as was checked on other ferroelectric materials with ordering near 50 K.

First, we measure our sample applying an electric field of 3.15 kV/cm (175 V). We show the induced polarization in Fig. 9 under the application of a 1-T magnetic field. We observe that the induced polarization has a broad maximum around 30 K. Above $T \approx 30$ K, the polarization decreases almost linearly and becomes zero near 70–75 K. The linear magnetolectric effect is observable only in the magnetically ordered phase. Thus it is surprising that the polarization disappears near 70–75 K while T_N is about 55 K. Thus we measure the induced polarization under $H=1$ T for a higher electric field. We show for comparison in the same figure, the induced polarization under 1-T magnetic field when applying a 4.5 kV/cm (250 V) electric field. The temperature behavior is similar for both electric fields. However, the polarization for a 4.5-kV/cm electric field becomes zero at a lower

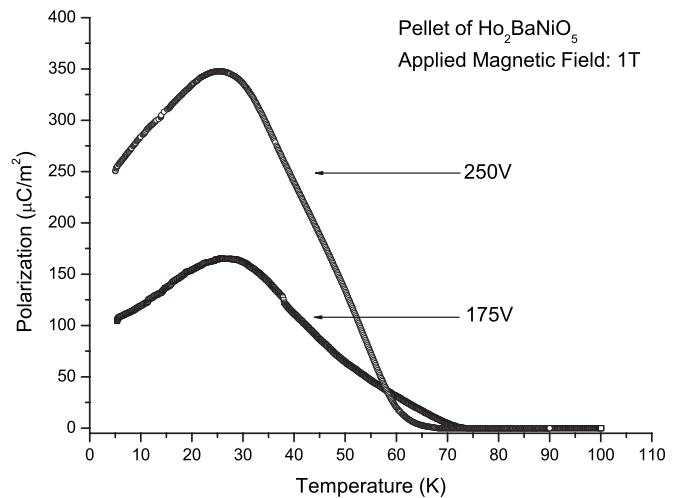


FIG. 9. Influence of the applied voltage on the induced polarization with $H=1$ T.

temperature around 60 K. Moreover, we notice a significantly higher value of the induced polarization for the 4.5-kV/cm electric field. Thus we believe that the apparent transition temperature to the paramagnetic paraelectric phase is related to the electric domains structure of our polycrystalline sample. One possible reason could be the presence of strong low dimensional interactions above T_N . This is known to occur in $\text{Nd}_2\text{BaNiO}_5$.¹⁸ The magnetic interactions could couple to the polarization and thus be affected by the strength of the electric field. Therefore the onset of the polarization does not coincide exactly with T_N .

Attempts of measurement with higher electric fields than 4.5 kV/cm were not possible due to the vicinity to the electrical breakdown of the sample. Consequently in the remaining part of our investigation, we made a magnetic field dependence study using a 4.5 kV/cm electric field. We present in Fig. 10 the magnetic field dependence of the induced polarization. There are common features of the induced polarization independent of the applied magnetic field. These common features are a linear dependence of the induced po-

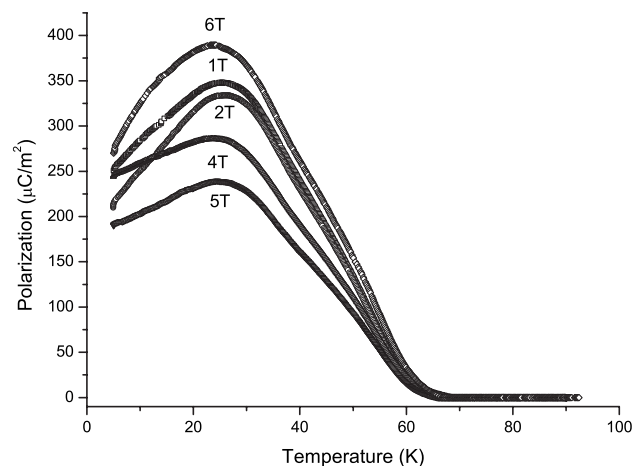


FIG. 10. Magnetic field dependence of the induced polarization measured on a pellet of $\text{Ho}_2\text{BaNiO}_5$ using a 4.5-kV/cm electric field.

larization close to T_N and a broad maximum around 30 K. In first approximation, we know that the induced polarization close to T_N is proportional to the magnetic order parameter.²¹ From neutron diffraction,¹³ we know that the Ho magnetic moment below T_N and over a quite large range of temperature has a quasilinear temperature dependence. The Ni moments saturate very quickly below T_N . Thus we ascribe the linear temperature dependence of the polarization below T_N as a result of the magnetic order parameter. In this temperature range, this magnetic order parameter is mostly governed by the Ho magnetic moment and thus we are not sensitive to the Haldane gap to which the Ni moments contribute. Another common feature is the broad maximum around 30 K which is almost magnetic field independent. This broad maximum is also present in the magnetic susceptibility (see Fig. 4) as a result of the one-dimensional character of the magnetic order. Thus we observe that the temperature dependence of the polarization reflects the 1D character of the magnetic order. Applying a magnetic field, we observe a decrease of the induced polarization from 1 to 5 T. At $H = 6$ T, we observe a jump in the induced polarization. This jump in the polarization can not be related to the eventual closing of the Haldane gap as discussed earlier. We know from susceptibility data that at H_{C2} , we have a new magnetic phase. Thus in the hypothesis of a higher magnetization, one can expect a higher induced polarization. If the gap is closed, then the total magnetic moment of the system would increase and thus the induced polarization would increase too. However, the decrease from 1 to 5 T followed by the increase at 6 T of the polarization remains to be explained. The obser-

vation of a finite polarization at any magnetic fields give us the indication that the three magnetic phases observed in Fig. 3 are magnetoelectric and thus magnetically ordered. This is surprising since the second metamagnetic phase transition at H_{C2} would typically give rise to a paramagnetic phase for a simple 1D-Heisenberg system. Additional measurements and neutron diffraction under magnetic field could clarify the magnetic field dependence of the structural and magnetic properties.

VI. CONCLUSION

Using symmetry arguments, we predict a linear magnetoelectric effect in $\text{Ho}_2\text{BaNiO}_5$. We investigate the magnetic and magnetoelectric properties of this Haldane gap system. We confirm the existence of two metamagnetic phase transitions at $H_{C1}=2.9$ T and at $H_{C2}=5.2$ T at 5 K. We show that this system presents a linear magnetoelectric effect which exhibits the 1D character of its magnetic order. In addition, we demonstrate the unusual magnetic behavior of this Heisenberg system through its magnetoelectric response. Further investigations are necessary to interpret the relationships between magnetic and dielectric properties.

ACKNOWLEDGMENTS

We acknowledge stimulating discussions with L.-P. Regnault. The work was supported by the Dutch National Science Foundation NWO, and by the breedtestrategieprogramma of the Materials Science Center, MSC⁺.

¹F. D. M. Haldane, Phys. Lett. **93A**, 464 (1983).

²L. P. Regnault, I. Zaliznyak, J. P. Renard, and C. Vettier, Phys. Rev. B **50**, 9174 (1994).

³J. P. Renard, M. Verdaguer, L.-P. Regnault, W. A. C. Erkelens, J. Rossat-Mignot, and W. G. Stirling, Europhys. Lett. **3**, 945 (1987); J. P. Renard, M. Verdaguer, L.-P. Regnault, W. A. C. Erkelens, J. Rossat-Mignot, J. Ribas, W. G. Stirling, and C. Vettier, J. Appl. Phys. **63**, 3538 (1988); K. Hirota, S. M. Shapiro, K. Katsumata, and M. Hagiwara, Physica B **213**, 173 (1995); J. P. Renard, L.-P. Regnault, and M. Verdaguer, J. Phys. (Paris), Colloq. **49**, 1425 (1988); A. Zheludev, S. E. Nagler, S. M. Shapiro, L. K. Chou, D. R. Talham, and M. W. Meisel, Phys. Rev. B **53**, 15004 (1996).

⁴J. Darriet and L. P. Regnault, Solid State Commun. **86**, 409 (1993).

⁵J. F. DiTusa, S.-W. Cheong, C. Broholm, G. Aeppli, L. W. Rupp, and B. Batlogg, Physica B **194-196**, 181 (1994); J. F. DiTusa, S.-W. Cheong, J. H. Park, G. Aeppli, C. Broholm, and C. T. Chen, Phys. Rev. Lett. **73**, 1857 (1994).

⁶S. T. Schiffer and H. K. Müller-Buschbaum, Z. Anorg. Allg. Chem. **540-541**, 243 (1986).

⁷J. Amador, E. Gutierrez-Puebla, M. A. Monge, I. Rasines, J. A. Campá, C. Ruiz-Valero, and J. M. Gomez de Salazar, Solid State Ionics **32-33**, 123 (1989).

⁸A. Salinas-Sánchez, R. Sáez-Puche, J. Rodríguez-Carvajal, and J. L. Martínez, Solid State Commun. **78**, 481 (1991).

⁹R. Sáez-Puche and S. R. Herrera Apéstigue, Ann. Chim. (Paris)

23, 415 (1998).

¹⁰A. Zheludev, J. M. Tranquada, T. Vogt, and D. J. Buttrey, Phys. Rev. B **54**, 6437 (1996), and references therein.

¹¹E. García-Matres, J. L. Martínez, and J. Rodríguez-Carvajal, Eur. Phys. J. B **24**, 59 (2001).

¹²H. T. Stokes and D. M. Hatch, ISOTROPY 2002, stokes.byu.edu/isotropy.html

¹³E. García-Matres, J. Rodríguez-Carvajal, and J. L. Martínez, Solid State Commun. **7**, 553 (1993).

¹⁴*Physical Properties of Crystals*, International Tables for Crystallography Vol. D, edited by A. Authier (Kluwer Academic Publishers, Dordrecht, 2003).

¹⁵A. C. Larson and R. B. Von Dreele, Los Alamos National Laboratory Report No. LAUR 86-748, 1994.

¹⁶S. Okubo, H. Ohta, T. Tanaka, T. Yokoo, and J. Akimitsu, Physica B **284-288**, 1475 (2000).

¹⁷E. García-Matres, J. L. García-Muñoz, J. L. Martínez, and J. Rodríguez-Carvajal, J. Magn. Magn. Mater. **149**, 363 (1995).

¹⁸A. Zheludev, S. Maslov, T. Yokoo, J. Akimitsu, S. Raymond, S. E. Nagler, and K. Hirota, Phys. Rev. B **61**, 11601 (2000).

¹⁹D. Poilblanc, H. Tsunetsugu, and T. M. Rice, Phys. Rev. B **50**, 6511 (1994); M. Troyer, H. Tsunetsugu, and D. Wurtz, *ibid.* **50**, 13515 (1994).

²⁰A. Zheludev, E. Ressouche, S. Maslov, T. Yokoo, S. Raymond, and J. Akimitsu, Phys. Rev. Lett. **80**, 3630 (1998).

²¹P. Tolédano, Ferroelectrics **161**, 257 (1994).